Channel Gain Lower Bound for IRS-assisted UAV-aided Communications

Giovanni Iacovelli (iD), *Graduate Student Member, IEEE*, Angelo Coluccia (iD), *Senior Member, IEEE* and Luigi Alfredo Grieco (iD), *Senior Member, IEEE*

Abstract—The Multiple-Input-Multiple-Output (MIMO) capabilities of an Intelligent Reflective Surface (IRS) combined with the inherent versatility of an Unmanned Aerial Vehicle (UAV) can significantly enhance the communication quality between a Ground User (GU) and a Base Station (BS). This work proposes a composite channel gain expression for performance analysis in IRS-assisted UAV-aided networks under Rician fading conditions. Differently from the present literature, the proposed formulation takes into account wave interference among surface elements and with the receiver. Moreover, Orthogonal Frequency Multiple Access (OFDMA) is employed to cope with spatial- and frequency-selective fading, enabling direct application in multiuser multi-drone scenarios. Numerical results demonstrate that the proposed model provides an underestimate, as expected from theoretical analysis, from which a lower bound for the data rate can be obtained, to be practically employed for system design and assessment.

Index Terms—IRS, UAV, Channel Modeling, Internet of Drones.

I. INTRODUCTION

UAVs are an important enabler for 5G and 6G communications and can be employed for a wide range of applications [1]. Recently, the scientific community considered the possibility to equip UAVs with IRSs, also known as Reconfigurable Intelligent Surfacess (RISs). IRSs are composed by Passive Reflective Units (PRUs) that can reflect and shift the incident electromagnetic wave by a programmable phase, thus yielding signal beamforming when optimally set. The high mobility of drones allows to change the IRS location to obtain a better Line of Sight (LoS) link and a lower pathloss. Although this combination grants a huge improvement of the channel quality, it comes with new challenges [2], [3] and in particular with the necessity of a dedicated channel model. This motivated recent studies that started to investigate the achievable performance of IRS-assisted UAV-aided systems, however existing approaches still neglect some important aspects.

In the very recent work [4], a thorough non-convex optimization framework is given to jointly design UAV trajectory, IRS's phase shifts, scheduling, and resource allocation, for
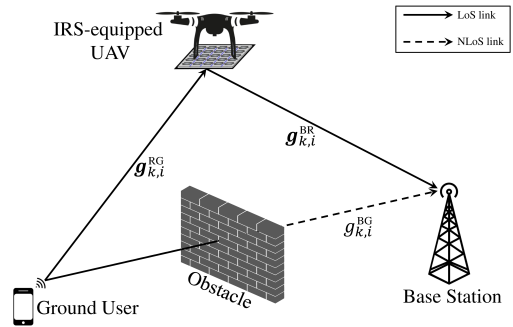
Fig. 1: Reference scenario.

an OFDMA communication system. However, only the LoS component is considered and hence a simplified deterministic channel model. A more accurate modeling is performed in [5], where closed-form approximations of outage probability, average symbol error probability, and channel capacity are derived for RIS-aided wireless networks over Rician fading channels. However, in this case the presence of a direct, yet weak, transmitter-receiver link is not considered. To fill this gap, [6] models such a link as a Rayleigh Random Variable (RV), by introducing a closed-form upper bound for the ergodic capacity, and a tight approximation for the outage probability. Moreover, simplified expressions in the asymptotic regime are also provided in [5], [6], motivated by the fact that the resulting distribution cannot be recast as a known one. In this respect, a stochastic model has been recently proposed in [7] in which IRSs are deployed for wireless multi-hop backhauling. The obtained channel gain expression is approximated to a Rician distribution and then evaluated in terms of outage and symbol error probability. However, in these works signal components are added coherently, thus neglecting wave interference among surface elements. Moreover, differently from [4], OFDMA is not considered hence multi-user transmission is not supported.

Motivated by the discussion above, this letter takes a step further towards the analytical development of a more comprehensive channel model for UAV-aided IRS-assisted OFDMA systems. In particular, it is envisioned a scenario in which a drone equipped with an IRS flies over the reference area to enhance the channel quality perceived by the BS, since the direct link between GU and BS may be too weak due to obstructions or unfavorable propagation, as depicted in Fig. 1. A stochastic channel model is derived, which takes into account interference between PRUs and GUs, and considers at the same time the presence of a weak LoS on the GU-

BS link. The obtained model provides an underestimate of the actual gain thus yielding a lower bound data rate that can be practically employed for system design and assessment. Moreover, it can be directly applied in multi-user multi-drone scenarios thanks to the adoption of OFDMA. To the best of the authors' knowledge, similar results are not available in the literature.

II. SYSTEM MODEL

A UAV is involved in a mission of duration T seconds, split in $k = 1, \ldots, K$ intervals of δ_t seconds. As a consequence, also the trajectory is discretized into a sequence of K locations denoted by $\mathbf{q}_k = [x_k^{\text{U}} \ y_k^{\text{U}} \ z_k^{\text{U}}]^{\mathsf{T}} \in \mathbb{R}^3$. Moreover, the UAV is equipped with an IRS composed by $M \times N$ PRUs. In each time interval k, each PRU of size s m^2 is assumed to reflect the incident signal with an amplitude $a_{k,m,n} \in [0,1]$ and a phase shift $\phi_{k,m,n} \in [0, 2\pi), m = 1, \ldots, M, n = 1, \ldots, N$, i.e., $\Gamma_{k,m,n} = a_{k,m,n}e^{j\phi_{k,m,n}}$. The centers of row elements are equally separated by d_r m, while column ones are spaced by d_c m. During the mission, the drone has to serve a GU, located at $\mathbf{w} = [x^{\text{G}}, y^{\text{G}}, z^{\text{G}}]^{\mathsf{T}} \in \mathbb{R}^3$, in order to enhance the communication channel with respect to a BS located at $\mathbf{q}^{\text{BS}} = [x^{\text{B}}, y^{\text{B}}, z^{\text{B}}]^{\mathsf{T}} \in \mathbb{R}^3$. Therefore, the distance between the GU and the BS is time invariant and described by $d^{\text{BG}} = \|\mathbf{q}^{\text{BS}} - \mathbf{w}\|$. On the contrary, UAV-GU and BS-UAV distances are time dependent and described by $d_k^{\text{RG}} = \|\mathbf{q}_k - \mathbf{w}\|$ and $d_k^{\text{BR}} = \|\mathbf{q}^{\text{BS}} - \mathbf{q}_k\|$, respectively.

The antennas of GU, BS, and IRS are characterized by power radiation pattern functions (including antenna gains) $F^{\text{GU}}(\theta, \varphi)$, $F^{\text{BS}}(\theta, \varphi)$, and $F^{\text{IRS}}(\theta, \varphi)$, respectively. These functions define the variation of the antennas' transmitted/received power along a certain direction in elevation and azimuth angles θ and φ. OFDMA is adopted by the whole wireless communication system, to avoid frequency interference with other GUs in the reference area. Therefore, the total bandwidth B is divided into subcarriers of δ_f Hz each. Without loss of generality, the GU can transmit on I subcarriers during the whole mission. Besides, it is assumed that the Channel State Information (CSI) is perfectly known at the BS.

The channel gain between the GU and the BS, in kth timeslot and subcarrier $i = 1, \ldots, I$ is

$$g_{k,i}^{\text{BG}} = \sqrt{\beta_0 d^{\text{BG}-\alpha} F^{\text{BG}}(\theta^{\text{BG}}, \varphi^{\text{BG}})} h_{k,i}^{\text{BG}}, \tag{1}$$

where β_0 denotes the channel power gain at the reference distance of 1 m, α is the pathloss exponent, $F^{\text{BG}}(\cdot, \cdot) = F^{\text{BS}}(\cdot, \cdot)F^{\text{GU}}(\cdot, \cdot)$, and $h_{k,i}^{\text{BG}} \sim \mathcal{CN}(\mu_{k,i}^{\text{BG}}, 2\sigma_{k,i}^{\text{BG}\,2})$ describes the channel coefficient. It is worth noting that the channel envelope $|h_{k,i}^{\text{BG}}|$ can be considered Rician [8], with K-factor $\kappa^{\text{BG}} = \frac{|\mu_{k,i}^{\text{BG}}|^2}{2\sigma_{k,i}^{\text{BG}\,2}}$ and average power $\Omega_{\text{BG}} = |\mu_{k,i}^{\text{BG}}|^2 + 2\sigma_{k,i}^{\text{BG}\,2} = 1$. Therefore, the channel coefficient can be modeled as

$$h_{k,i}^{\text{BG}} = \sqrt{\frac{\kappa^{\text{BG}}}{\kappa^{\text{BG}}+1}} \overline{h}_{k,i}^{\text{BG}} + \sqrt{\frac{1}{\kappa^{\text{BG}}+1}} \widetilde{h}_{k,i}^{\text{BG}}. \tag{2}$$

In particular, $\overline{h}_{k,i}^{\text{BG}} = e^{-j2\pi i \delta_f \frac{d^{\text{BG}}}{c}}$ is the LoS component, $j = \sqrt{-1}$, characterized by a phase shift depending on the user's subcarrier index, while $\widetilde{h}_{k,i}^{\text{BG}}[n] \sim \mathcal{CN}(0,1)$ is circular symmetric Gaussian distributed, describing small-scale fading.

Similarly, UAV-GU channel gain in timeslot k, subcarrier i, between GU and UAV, is modeled as follows:

$$\mathbf{g}_{k,i}^{\text{RG}} = \sqrt{\beta_0 d_k^{\text{RG}-\alpha} F^{\text{RG}}(\theta_k^{\text{RG}}, \varphi_k^{\text{RG}})} \mathbf{h}_{k,i}^{\text{RG}}, \tag{3}$$

$$\mathbf{h}_{k,i}^{\text{RG}} = \sqrt{\frac{\kappa^{\text{RG}}}{\kappa^{\text{RG}}+1}} \overline{\mathbf{h}}_{k,i}^{\text{RG}} + \sqrt{\frac{1}{\kappa^{\text{RG}}+1}} \widetilde{\mathbf{h}}_{k,i}^{\text{RG}}, \tag{4}$$

$$\overline{\mathbf{h}}_{k,i}^{\text{RG}} = e^{-j2\pi i \delta_f \frac{d_k^{\text{RG}}}{c}} \mathbf{h}_{k,\text{LoS}}^{\text{RG}}, \tag{5}$$

and $F^{\text{RG}}(\cdot, \cdot) = F^{\text{IRS}}(\cdot, \cdot)F^{\text{GU}}(\cdot, \cdot)$. Moreover, $\mathbf{h}_{k,\text{LoS}}^{\text{RG}}$ denotes the far-field array response [4] defined as

$$\mathbf{h}_{k,\text{LoS}}^{\text{RG}} \in \mathbb{C}^{MN \times 1} =$$

$$\left[1 \ e^{-j2\pi f_c \frac{d_r \sin\theta_k^{\text{RG}} \cos\varphi_k^{\text{RG}}}{c}} \ \cdots \ e^{-j2\pi f_c \frac{(M-1)d_r \sin\theta_k^{\text{RG}} \cos\varphi_k^{\text{RG}}}{c}} \right]^{\mathsf{T}}$$

$$\otimes \left[1 \ e^{-j2\pi f_c \frac{d_c \sin\theta_k^{\text{RG}} \sin\varphi_k^{\text{RG}}}{c}} \ \cdots e^{-j2\pi f_c \frac{(N-1)d_c \sin\theta_k^{\text{RG}} \sin\varphi_k^{\text{RG}}}{c}} \right]^{\mathsf{T}}, \tag{6}$$

where $\widetilde{\mathbf{h}}_{k,i}^{\text{RG}} \sim \mathcal{CN}(0, \mathbf{I}_{MN})$ and $\otimes$ denotes the Kronecker product. It is worth noting that, with respect to (2), one more phase shift affects the channel model which depends on the vertical and horizontal Angles of Arrival (AoA) of the signal, i.e., θ_k^{RG} and φ_k^{RG}. In particular, $\sin\theta_k^{\text{RG}} = \frac{|z_k^{\text{U}}-z^{\text{G}}|}{d_k^{\text{RG}}}$, $\sin\varphi_k^{\text{RG}} = \frac{|x_k^{\text{U}}-x^{\text{G}}|}{\sqrt{(x_k^{\text{U}}-x^{\text{G}})^2+(y_k^{\text{U}}-y^{\text{G}})^2}}$, and $\cos\varphi_k^{\text{RG}} = \frac{|y^{\text{G}}-y_k^{\text{U}}|}{\sqrt{(x_k^{\text{U}}-x^{\text{G}})^2+(y_k^{\text{U}}-y^{\text{G}})^2}}$. Finally, the channel gain of UAV-BS link, $\forall k$ and $\forall i$, is

$$\mathbf{g}_{k,i}^{\text{BR}} = \sqrt{\beta_0 s d_k^{\text{BR}-\alpha} F^{\text{BR}}(\theta_k^{\text{BR}}, \varphi_k^{\text{BR}})} \mathbf{h}_{k,i}^{\text{BR}}, \tag{7}$$

$$\mathbf{h}_{k,i}^{\text{BR}} = \sqrt{\frac{\kappa^{\text{BR}}}{\kappa^{\text{BR}}+1}} \overline{\mathbf{h}}_{k,i}^{\text{BR}} + \sqrt{\frac{1}{\kappa^{\text{BR}}+1}} \widetilde{\mathbf{h}}_{k,i}^{\text{BR}}, \tag{8}$$

$$\overline{\mathbf{h}}_{k,i}^{\text{BR}} = e^{-j2\pi i \delta_f \frac{d_k^{\text{BR}}}{c}} \mathbf{h}_{k,\text{LoS}}^{\text{BR}}, \tag{9}$$

$F^{\text{BR}}(\cdot, \cdot) = F^{\text{BS}}(\cdot, \cdot)F^{\text{IRS}}(\cdot, \cdot)$, while θ_k^{RG} and φ_k^{RG} are the vertical and horizontal Angles of Departure (AoD), respectively, so that $\sin\theta_k^{\text{BR}} = \frac{|z_k^{\text{U}}-z^{\text{B}}|}{d_k^{\text{BR}}}$, $\sin\varphi_k^{\text{BR}} = \frac{|x_k^{\text{U}}-x^{\text{B}}|}{\sqrt{(x_k^{\text{U}}-x^{\text{B}})^2+(y_k^{\text{U}}-y^{\text{B}})^2}}$, and $\cos\varphi_k^{\text{BR}} = \frac{|y^{\text{B}}-y_k^{\text{U}}|}{\sqrt{(x_k^{\text{U}}-x^{\text{B}})^2+(y_k^{\text{U}}-y^{\text{B}})^2}}$. Finally, similarly to (6),

$$\mathbf{h}_{k,\text{LoS}}^{\text{BR}} \in \mathbb{C}^{MN \times 1} =$$

$$\left[1 \ e^{-j2\pi f_c \frac{d_r \sin\theta_k^{\text{BR}} \cos\varphi_k^{\text{BR}}}{c}} \ \cdots \ e^{-j2\pi f_c \frac{(M-1)d_r \sin\theta_k^{\text{BR}} \cos\varphi_k^{\text{BR}}}{c}} \right]^{\mathsf{T}}$$

$$\otimes \left[1 \ e^{-j2\pi f_c \frac{d_c \sin\theta_k^{\text{BR}} \sin\varphi_k^{\text{BR}}}{c}} \ \cdots e^{-j2\pi f_c \frac{(N-1)d_c \sin\theta_k^{\text{BR}} \sin\varphi_k^{\text{BR}}}{c}} \right]^{\mathsf{T}},$$

and $\widetilde{\mathbf{h}}_{k,i}^{\text{BR}} \sim \mathcal{CN}(0, \mathbf{I}_{MN})$. The IRS phase shift matrix $\mathbf{\Phi}_k \in \mathbb{C}^{MN \times MN}$, for each timeslot k, is defined as

$$\mathbf{\Phi}_k = \text{diag}\Big(a_{k,1,1}e^{j\phi_{k,1,1}}, \ldots, a_{k,1,N}e^{j\phi_{k,1,N}}, \ldots,$$

$$a_{k,M,1}e^{j\phi_{k,M,1}}, \ldots, a_{k,M,N}e^{j\phi_{k,M,N}} \Big), \tag{10}$$

and, hence, the composite IRS UAV-assisted channel gain between GU and BS in subcarrier i is

$$G_{k,i} = \mathbf{g}_{k,i}^{\text{BR}\,\mathsf{T}} \mathbf{\Phi}_k \mathbf{g}_{k,i}^{\text{RG}} + g_{k,i}^{\text{BG}}. \tag{11}$$

Recalling Shannon's equation, the channel capacity in timeslot k and subcarrier i is thus given by

$$C_{k,i} = \delta_f \log_2 \left(1 + \frac{P_{k,i} |G_{k,i}|^2}{\rho^2} \right), \tag{12}$$

where $P_{k,i}$ is the transmit power of GUs in i-th subcarrier and $\rho^2 = N_0 \delta_f$ is the noise power, whereas N_0 denotes the spectral noise power. Given a maximum achievable data rate $R_{k,i}$, to guarantee a reliable communication, it is required that the outage probability $p_{k,i}$ remains below a threshold ε, i.e.

$$p_{k,i} = \mathbb{P}\left(C_{k,i} < R_{k,i} \right) = \mathbb{P}\left(|G_{k,i}|^2 < \frac{\rho^2(2^{\frac{R_{k,i}}{\delta_f}} - 1)}{P_{k,i}} \right)$$

$$= F_{|G_{k,i}|^2}\left(\frac{\rho^2(2^{\frac{R_{k,i}}{\delta_f}} - 1)}{P_{k,i}} \right) \le \varepsilon, \ \forall \ \begin{array}{l} k = 1, \ldots, K, \\ i = 1, \ldots, I, \end{array}$$

with $F_{|G_{k,i}|^2}$ denoting the Cumulative Distribution Function (CDF) of $|G_{k,i}|^2$. Therefore, considering the maximum tolerable outage, i.e., $p_{k,i} = \varepsilon$, the data rate is obtained as

$$R_{k,i} = \delta_f \log_2 \left(1 + \underbrace{\frac{P_{k,i} \ F^{-1}_{|G_{k,i}|^2}(\varepsilon)}{\rho^2}}_{\text{Signal-to-Noise Ratio (SNR)}} \right). \tag{13}$$

Unfortunately, a closed-form expression of $F_{|G_{k,i}|^2}$ is difficult to calculate. Indeed, $G_{k,i}$ involves the pairwise product of two complex Gaussian RVs, whose distribution, named complex double Gaussian, is given in terms of an infinite sum of modified Bessel functions [9], hence intractable for the sake of the present analysis. Besides, dealing with the square module of the summation in (11) is even more challenging. Therefore, an approximation is useful to handle with such a scenario.

III. Channel Modeling Approximation

In this Section an approximation of the composite channel model is provided. Fixed (m,n), i, and k, let $h^{\text{BR}}_{k,i,m,n} \sim \mathcal{CN}(\mu^{\text{BR}}_{k,i,m,n}, 2\sigma^{\text{BR}\,2}_{k,i,m,n})$ and $h^{\text{RG}}_{k,i,m,n} \sim \mathcal{CN}(\mu^{\text{RG}}_{k,i,m,n}, 2\sigma^{\text{RG}\,2}_{k,i,m,n})$ be two generic channel gains related to BS-PRU-GU link $h^{\text{BRG}}_{k,i,m,n}$ where, similarly to (2) and related definitions, the following relationship are obtained:

$$\mu^{\text{BR}}_{k,i,m,n} = \sqrt{\frac{\kappa^{\text{BR}}}{\kappa^{\text{BR}} + 1}} e^{-j2\pi i \delta_f \frac{d^{\text{BR}}_k}{c}}$$
$$\times e^{-j2\pi f_c \frac{(m-1)d_r \sin\theta^{\text{BR}}_k \cos\varphi^{\text{BR}}_k + (n-1)d_c \sin\theta^{\text{BR}}_k \sin\varphi^{\text{BR}}_k}{c}}, \tag{14}$$

$$\mu^{\text{RG}}_{k,i,m,n} = \sqrt{\frac{\kappa^{\text{RG}}}{\kappa^{\text{RG}} + 1}} e^{-j2\pi i \delta_f \frac{d^{\text{RG}}_k}{c}}$$
$$\times e^{-j2\pi f_c \frac{(m-1)d_r \sin\theta^{\text{RG}}_k \cos\varphi^{\text{RG}}_k + (n-1)d_c \sin\theta^{\text{RG}}_k \sin\varphi^{\text{RG}}_k}{c}}, \tag{15}$$

$$2\sigma^{\text{BR}\,2} = \frac{1}{\kappa^{\text{BR}} + 1}, \qquad 2\sigma^{\text{RG}\,2} = \frac{1}{\kappa^{\text{RG}} + 1}. \tag{16}$$

The product $h^{\text{BR}}_{k,i,m,n} h^{\text{RG}}_{k,i,m,n}$ is distributed as a complex double Gaussian that however, as mentioned, is difficult to handle. The following Lemma provides an approximation that is useful for the subsequent development.

Lemma 1. *Given* (m,n), i, *and* k, *the product* $h^{\text{BR}}_{k,i,m,n} h^{\text{RG}}_{k,i,m,n}$ *can be approximated by a complex Gaussian variable* $Z_{k,i,m,n} \sim \mathcal{CN}(\mu^Z_{k,i,m,n}, 2\sigma^{Z}_{k,i,m,n}{}^2)$ *with* $\mu^Z_{k,i,m,n} = \mu^{\text{BR}}_{k,i,m,n}\mu^{\text{RG}}_{k,i,m,n}$ *and* $2\sigma^Z_{k,i,m,n}{}^2 = 2\sigma^{\text{RG}}_{k,i,m,n}{}^2|\mu^{\text{BR}}_{k,i,m,n}|^2 + 2\sigma^{\text{BR}}_{k,i,m,n}{}^2|\mu^{\text{RG}}_{k,i,m,n}|^2$.

Proof. For brevity, let $h_{\text{BR}} \triangleq h^{\text{BR}}_{k,i,m,n}$ and $h_{\text{RG}} \triangleq h^{\text{RG}}_{k,i,m,n}$. The product is defined as $Z \triangleq h_{\text{BR}} h_{\text{RG}} = Z^{\text{R}} + jZ^{\text{I}}$, where the real and imaginary parts are $Z^{\text{R}} = h^{\text{R}}_{\text{BR}} h^{\text{R}}_{\text{RG}} - h^{\text{I}}_{\text{BR}} h^{\text{I}}_{\text{RG}}$ and $Z^{\text{I}} = h^{\text{R}}_{\text{BR}} h^{\text{I}}_{\text{RG}} + h^{\text{I}}_{\text{BR}} h^{\text{R}}_{\text{RG}}$. In particular, $\{h^{\text{R}}_{\text{BR}}, h^{\text{R}}_{\text{RG}}, h^{\text{I}}_{\text{BR}}, h^{\text{I}}_{\text{RG}}\} \sim \mathcal{N}\left(\{m^{\text{R}}_{\text{BR}}, m^{\text{R}}_{\text{RG}}, m^{\text{I}}_{\text{BR}}, m^{\text{I}}_{\text{RG}}\}, \{\sigma^2_{\text{BR}}, \sigma^2_{\text{RG}}, \sigma^2_{\text{BR}}, \sigma^2_{\text{RG}}\}\right)$. The product of two independent Gaussian RVs $X \sim \mathcal{N}(m_X, \sigma_X{}^2)$ and $Y \sim \mathcal{N}(m_Y, \sigma_Y{}^2)$ has the following statistics [10]

$$\mathbb{E}[XY] = m_X m_Y,$$
$$\mathbb{E}[(XY - \mathbb{E}[XY])^2] = m_Y^2 \sigma_X^2 + (m_X^2 + \sigma_X^2)\sigma_Y^2$$
$$= (1 + \delta_X^2 + \delta_Y^2)\sigma_X^2 \sigma_Y^2,$$

where $\delta_X = \frac{m_X}{\sigma_X}$ and $\delta_Y = \frac{m_Y}{\sigma_Y}$. The distribution of XY tends to $\mathcal{N}(m_X m_Y, m_X^2 \sigma_Y^2 + m_Y^2 \sigma_X^2)$ for $\{\delta_X, \delta_Y\} \gg 1$, hence the following inequality holds

$$\mathbb{E}[(XY - \mathbb{E}[XY])^2] > m_X^2 \sigma_Y^2 + m_Y^2 \sigma_X^2. \tag{17}$$

The statistics of Z^{R} and Z^{I} are:

$$m^{\text{R}}_Z = m^{\text{R}}_{\text{BR}} m^{\text{R}}_{\text{RG}} - m^{\text{I}}_{\text{BR}} m^{\text{I}}_{\text{RG}}, \quad m^{\text{I}}_Z = m^{\text{R}}_{\text{BR}} m^{\text{I}}_{\text{RG}} + m^{\text{R}}_{\text{RG}} m^{\text{I}}_{\text{BR}},$$
$$\sigma^{\text{R}}_Z{}^2 = \sigma^{\text{I}}_Z{}^2 = \sigma^2_{\text{RG}} m^{\text{R}}_{\text{BR}}{}^2 + \sigma^2_{\text{BR}} m^{\text{R}}_{\text{RG}}{}^2 + \sigma^2_{\text{RG}} m^{\text{I}}_{\text{BR}}{}^2 + \sigma^2_{\text{BR}} m^{\text{I}}_{\text{RG}}{}^2 \triangleq \sigma^2_Z.$$

Finally, the first and second central moments of $Z \sim \mathcal{CN}(\mu_Z, 2\sigma_Z{}^2)$ are

$$\mu_Z = m^{\text{R}}_Z + jm^{\text{I}}_Z = (m^{\text{R}}_{\text{BR}} + jm^{\text{I}}_{\text{BR}})(m^{\text{R}}_{\text{RG}} + jm^{\text{I}}_{\text{RG}}) = \mu_{\text{BR}}\mu_{\text{RG}}$$
$$2\sigma_Z^2 = \sigma^{\text{R}}_Z{}^2 + \sigma^{\text{I}}_Z{}^2 = 2\sigma^2_{\text{RG}}|\mu_{\text{BR}}|^2 + 2\sigma^2_{\text{BR}}|\mu_{\text{RG}}|^2,$$

hence the thesis is proven. ∎

Remark 1. *From* (17), *it follows that the Probability Density Function (PDF) of the provided approximation* $Z_{k,i,m,n}$ *has lower variance than the actual (complex double Gaussian) PDF of* $h^{\text{BR}}_{k,i,m,n} h^{\text{RG}}_{k,i,m,n}$. *Moreover, considering also that the latter is positively-skewed* [10, Eq. (33)], *intuitively, it can be expected that the tail of the approximated PDF decays faster than the actual one. This in turn means that the Inverse CDF of* $Z_{k,i,m,n}$ *is expected to provide a lower bound, for sufficiently high probability values. Such an intuition will be confirmed by the numerical results in Section IV.*

From Lemma 1, it results that $h^{\text{BRG}}_{k,i,m,n} = Z_{k,i,m,n}\Gamma_{k,m,n} \sim \mathcal{CN}(\mu^{\text{BRG}}_{k,i,m,n}, 2\sigma^{\text{BRG}\,2}_{k,i,m,n})$ where, to ease the notation, (14)-(15) have been rewritten as $\mu^{\text{BR}}_{k,i,m,n} = \sqrt{\frac{\kappa^{\text{BR}}}{\kappa^{\text{BR}}+1}} e^{j\psi^{\text{BR}}_{k,i,m,n}}$ and $\mu^{\text{RG}}_{k,i,m,n} = \sqrt{\frac{\kappa^{\text{RG}}}{\kappa^{\text{RG}}+1}} e^{j\psi^{\text{RG}}_{k,i,m,n}}$, with obvious definition of the phase terms. Hence, the envelope $|h^{\text{BRG}}_{k,i,m,n}|$ can be considered a Rician RV, leading to the model of the same type as in (2), (4) or (8), i.e.

$$h^{\text{BRG}}_{k,i,m,n} = a_{k,m,n}\left(\sqrt{\overline{\kappa}^{\text{BRG}}} e^{j\Psi_{k,i,m,n}} + \sqrt{\widetilde{\kappa}^{\text{BRG}}} \widetilde{h}^{\text{BRG}} \right), \tag{18}$$

$$\nu^2_{G_{k,i}} = \eta_k^2 \overline{\kappa}^{\text{BRG}} \left(2 \sum_{z>z'}^{MN} a_{k,z} a_{k,z'} \cos\left(\Psi_z - \Psi_{z'}\right) + \sum_{z=1}^{MN} a_{k,z}^2 \right) + \lambda\sqrt{\kappa^{\text{BG}}} \left(2\eta_k \sqrt{\overline{\kappa}^{\text{BRG}}} \sum_{z=1}^{MN} a_{k,z} \cos\left(\psi_i^{\text{BG}} - \Psi_z\right) + \lambda\sqrt{\kappa^{\text{BG}}} \right) \quad (23)$$

where $\widetilde{h}^{\text{BRG}} \sim \mathcal{CN}(0,1)$ and, recalling that $\Gamma_{k,m,n} = a_{k,m,n} e^{j\phi_{k,m,n}}$ with amplitude $a_{k,m,n}$ and phase shift $\phi_{k,m,n}$,

$$\overline{\kappa}^{\text{BRG}} = \frac{\kappa^{\text{BR}}\kappa^{\text{RG}}}{(\kappa^{\text{BR}}+1)(\kappa^{\text{RG}}+1)}, \quad \widetilde{\kappa}^{\text{BRG}} = \frac{\kappa^{\text{BR}}+\kappa^{\text{RG}}}{(\kappa^{\text{BR}}+1)(\kappa^{\text{RG}}+1)},$$

with $\Psi_{k,i,m,n} = \phi_{k,m,n} + \psi_{k,i,m,n}^{\text{BR}} + \psi_{k,i,m,n}^{\text{RG}}$. Notice that phase terms are irrelevant to the scatter component [4].

Once the expression of generic PRU-related cascaded channel has been obtained, it is necessary to derive a tractable expression for the UAV-aided IRS-assisted channel model.

Theorem 1. *Given k and i, the channel envelope $|G_{k,i}|$ of the whole system has approximately a Rician distribution characterized by K-factor $\kappa = \frac{\nu^2_{G_{k,i}}}{2\sigma^2_{G_{k,i}}}$ and average power $\Omega = \nu^2_{G_{k,i}} + 2\sigma^2_{G_{k,i}}$, with $\nu^2_{G_{k,i}}$ defined in (23) (at the top of this page) and $2\sigma^2_{G_{k,i}} = \eta_k^2 \widetilde{\kappa}^{\text{BRG}} \sum_{z=1}^{MN} a_{k,z}^2 + \lambda^2 \widetilde{\kappa}^{\text{BG}}$.*

Proof. By using the BS-GU link in (1) and combining the expressions in Section II with the result (18) derived in Lemma 1, (11) can be rewritten as

$$G_{k,i} = \eta_k \sum_{m=1}^{M} \sum_{n=1}^{N} h_{k,i,m,n}^{\text{BRG}} + \lambda h_{k,i}^{\text{BG}}, \quad (19)$$

where $\eta_k = \beta_0 \sqrt{(d_k^{\text{BR}} d_k^{\text{RG}})^{-\alpha}} s F^{\text{BRG}}(\theta_k^{\text{BR}}, \varphi_k^{\text{BR}}, \theta_k^{\text{RG}}, \varphi_k^{\text{RG}})$, $\lambda = \sqrt{\beta_0 d^{\text{BG}-\alpha} F^{\text{BG}}(\theta^{\text{BG}}, \varphi^{\text{BG}})}$, and $F^{\text{BRG}}(\cdot,\cdot,\cdot,\cdot) = F^{\text{BR}}(\cdot,\cdot) F^{\text{RG}}(\cdot,\cdot)$. Since $G_{k,i} = G_{k,i}^{\text{R}} + j G_{k,i}^{\text{I}}$, where $\{G_{k,i}^{\text{R}}, G_{k,i}^{\text{I}}\} \sim \mathcal{N}(\{\mu_{G_{k,i}}^{\text{R}}, \mu_{G_{k,i}}^{\text{I}}\}, \{\sigma^2_{G_{k,i}}, \sigma^2_{G_{k,i}}\})$, it results

$$\mu_{G_{k,i}}^{\text{R}} = \eta_k \sqrt{\overline{\kappa}^{\text{BRG}}} \sum_{m=1}^{M} \sum_{n=1}^{N} a_{k,m,n} \cos\Psi_{k,i,m,n} + \lambda\sqrt{\overline{\kappa}^{\text{BG}}} \cos\psi_i^{\text{BG}},$$

$$\mu_{G_{k,i}}^{\text{I}} = \eta_k \sqrt{\overline{\kappa}^{\text{BRG}}} \sum_{m=1}^{M} \sum_{n=1}^{N} a_{k,m,n} \sin\Psi_{k,i,m,n} + \lambda\sqrt{\overline{\kappa}^{\text{BG}}} \sin\psi_i^{\text{BG}},$$

where $\overline{\kappa}^{\text{BG}} = \frac{\kappa^{\text{BG}}}{\kappa^{\text{BG}}+1}$ and $\psi_i^{\text{BG}} = -2\pi i \delta_f \frac{d^{\text{BG}}}{c}$. For all m and n, define $\{z, z'\} = (m,n)$ as the linearized indexes of IRS elements. The corresponding squared LoS component $\nu^2_{G_{k,i}} = {\mu_{G_{k,i}}^{\text{R}}}^2 + {\mu_{G_{k,i}}^{\text{I}}}^2$ is given in (23) (at the top of this page). Moreover, the Non Line of Sight (NLoS) component is $2\sigma^2_{G_{k,i}} = \eta_k^2 \widetilde{\kappa}^{\text{BRG}} \sum_{z=1}^{MN} a_{k,z}^2 + \lambda^2 \widetilde{\kappa}^{\text{BG}}$, i.e., the sum of all scatter components involved in the system. ∎

Corollary 1. *The effective data rate (13) can be directly derived by computing the fading-power $F_{|G_{k,i}|^2}^{-1}$, which can be easily calculated as in [11].*

Corollary 2. *The obtained channel gain can be specialized for the case of Rayleigh fading by considering in (23) a completely obstructed BS-GU link, i.e., $\overline{\kappa}^{BG} \to 0$.*

Remark 2. *Following the lead of [7, Sec. III.C], it is not difficult to show that $|G_{k,i}|^2$ scales as $(M \times N)^2$. Thus,*

increasing the size of the IRSs greatly improves the fading-power, and hence SNR, so significantly lowering the outage probability, as shown in the next Section.

It is worth noting that (23), which can be easily extended to scenarios in which multiple IRSs are present, exhibits two wave interference patterns: the former related to constructive/destructive superposition of the received waves among PRUs, the latter related to the coupling between each IRS element and the GU. Note also that (23) remains valid also for discrete phase shifts. In that case, however, it cannot be guaranteed that (23) is maximized, since cosine patterns may not be equal to 1. This leads to a performance degradation of the system that strictly depends on the phase quantization level. Notice that a similar effect may also arise from other causes, e.g. jitter. Still, the system is robust against the resulting beam-pointing degradation, since the elevation of the UAV yields a favorable ground illumination footprint. The accuracy of the provided approximation in Theorem 1 indirectly depends on two parameters δ_X and δ_Y involved in the approximation of $Z_{k,i,m,n}$, which are the reciprocals of the coefficient of variation for the variables X and Y defined in the proof of Lemma 1. This translates to a gap in $F_{|G_{k,i}|^2}^{-1}$, which reduces when the link is dominated by the LoS component, i.e., $\{\kappa^{\text{BR}}, \kappa^{\text{RG}}\} \gg 1$. This has been proved to be the case for Air-to-Ground (A2G), and thus UAV-aided, communications [4], hence the ultimately provided lower bound on the outage probability is tight in such a regime, typical of UAV-assisted scenarios, as shown below by means of numerical simulations.

IV. NUMERICAL RESULTS AND DISCUSSION

The obtained model is mainly affected by the error introduced by approximating the product of two complex Normal RV as a complex Normal instead of a complex double Gaussian, as discussed in Section III. To validate its accuracy, three parameter settings are considered, i.e., $\delta_X = \delta_Y = \{1, 2, 3\}$. Results for 10^6 realizations are depicted in Fig. 2.
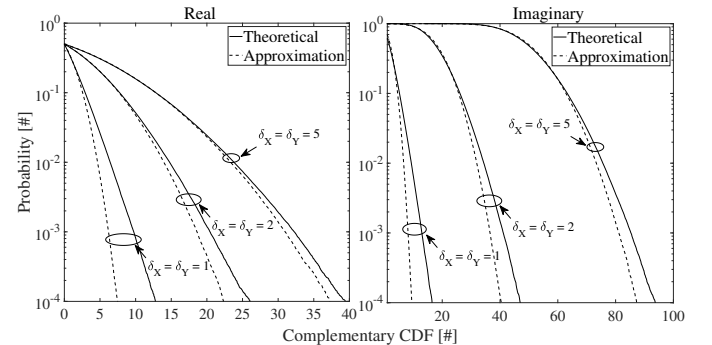

Fig. 2: Comparison between approximation and actual Complementary CDF for different values of δ_X and δ_Y.
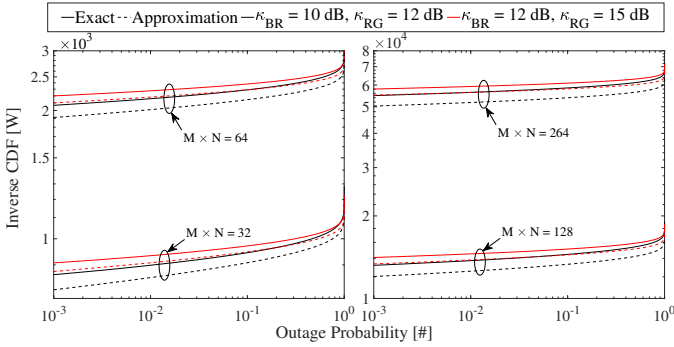
Fig. 3: $F_{|G_{k,i}|^2}^{-1}$ for different K-factors and number of PRUs.

It clearly emerges that for higher values of $\{\delta_X, \delta_Y\}$ the distance between theoretical and approximation curves reduces. Specifically, the approximation underestimates the actual value in both real and imaginary parts, thus confirming Remark 1. Consequently, depending on $\{\delta_X, \delta_Y\}$, the approximation errors accumulated in (19) will translate into a certain underestimation error in $F_{|G_{k,i}|^2}^{-1}$. From a physical meaning perspective, the values of $\{\delta_X, \delta_Y\}$ are proportional to the power of the LoS, which in turn is related to the Rician K-factors. Given that in practical UAV-assisted communications the latter are between 5 dB and 15 dB [11], the provided approximation remains satisfactory also for very small probability.

Numerical results, based on 5×10^5 realizations, are now provided to get insights about the proposed model. Without loss of generality, consider a fixed instant k in which the optimal phase shift matrix $\mathbf{\Phi}_k$ is applied such that unitary cosine patterns in (23) are obtained. According to [11], in all configurations the BS-GU link has a weaker LoS component, i.e., $\kappa^{\text{BG}} = 6$ dB, than BS-UAV and UAV-GU links, for which $\kappa^{\text{BR}} = \{10, 12\}$ dB and $\kappa^{\text{RG}} = \{12, 15\}$ dB. Several numbers of PRUs of the IRS are considered $M \times N = \{32, 64, 128, 256\}$ and the coefficients $\{\eta_k, \lambda\}$ are normalized to unity as in [7], thus not depend on the position-related parameters, which are hence left unspecified.

Fig. 3 confirms that the proposed channel gain model leads to a lower bound on the outage probability. This result, following Corollary 1, can be practically used to determine a conservative, but fairly tight data rate level for system pro-
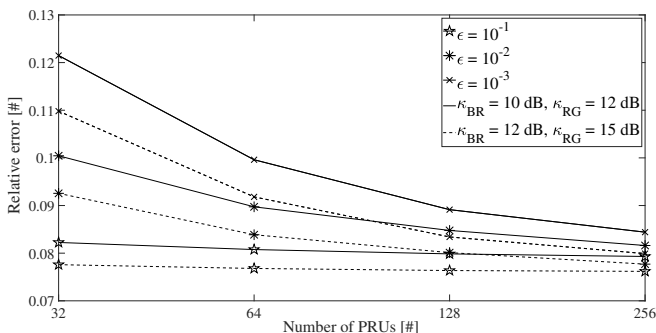
visioning and optimization. In particular, it can be noticed that the distance between exact (solid) and approximate (dashed) fading-power curves is lower when the K-factors increase, for all values of the number of PRUs $M \times N$. From a physical meaning perspective, this reflects the fact that the BS-UAV-GU link is mostly in LoS condition. Thus, as discussed, for typical Rician factors values the approximation of the double Gaussian distribution is quite accurate so yielding, in turn, a good accuracy in the fading-power approximation. To better highlight this fact, Fig. 4 shows the relative error between the exact and approximate curves depicted in Fig. 3, for different values of the outage probability, i.e., $\varepsilon = \{10^{-1}, 10^{-2}, 10^{-3}\}$. It can be observed that the relative error decreases with the number of PRUs, which clearly indicates that a larger RIS provides better signal reflection and, hence, is beneficial to the ultimate performance. For instance, $M \times N = 128$ elements already achieve a remarkable 8.5% approximation error, for $\kappa^{\text{BR}} = 10$ dB, $\kappa^{\text{RG}} = 12$ dB, and $\varepsilon = 10^{-2}$.

V. Conclusions

An approximation for the channel gain in IRS-assisted UAV-aided networks has been derived. The model considers the presence of (i) a weak LoS link between GU and a BS, and (ii) frequency and spatial selective fading. The proposed approximation ultimately provides a data rate lower bound, as corroborated by numerical results, which can be practically used to determine a conservative, but fairly tight data rate level. Future works include the optimization of UAVs trajectories and phase matrices.

References

[1] P. Boccadoro, D. Striccoli, and L. A. Grieco, "An extensive survey on the internet of drones," *Ad Hoc Netw.*, vol. 122, p. 102600, 2021.

[2] A. S. Abdalla, T. F. Rahman, and V. Marojevic, "UAVs with Reconfigurable Intelligent Surfaces: Applications, Challenges, and Opportunities," 2020. [Online]. Available: https://arxiv.org/abs/2012.04775

[3] B. Shang, R. Shafin, and L. Liu, "UAV Swarm-Enabled Aerial Reconfigurable Intelligent Surface," 2021. [Online]. Available: https://arxiv.org/abs/2103.06361

[4] Z. Wei, Y. Cai, Z. Sun, D. W. K. Ng, J. Yuan, M. Zhou, and L. Sun, "Sum-Rate Maximization for IRS-Assisted UAV OFDMA Communication Systems," *IEEE Trans. Wireless Commun.*, vol. 20, no. 4, pp. 2530–2550, 2021.

[5] Q. Tao, J. Wang, and C. Zhong, "Performance Analysis of Intelligent Reflecting Surface Aided Communication Systems," *IEEE Commun. Lett.*, vol. 24, no. 11, pp. 2464–2468, 2020.

[6] A. M. Salhab and M. H. Samuh, "Accurate Performance Analysis of Reconfigurable Intelligent Surfaces Over Rician Fading Channels," *IEEE Wireless Commun. Lett.*, vol. 10, no. 5, pp. 1051–1055, 2021.

[7] M. A. Al-Jarrah, E. Alsusa, A. Al-Dweik, and M.-S. Alouini, "Performance Analysis of Wireless Mesh Backhauling Using Intelligent Reflecting Surfaces," *IEEE Trans. Wireless Commun.*, 2021.

[8] M. A. Al-Jarrah, K.-H. Park, A. Al-Dweik, and M.-S. Alouini, "Error Rate Analysis of Amplitude-Coherent Detection over Rician Fading Channels with Receiver Diversity," *IEEE Trans. Wireless Commun.*, vol. 19, no. 1, pp. 134–147, 2019.

[9] N. O'Donoughue and J. M. F. Moura, "On the Product of Independent Complex Gaussians," *IEEE Trans. Signal Process*, vol. 60, no. 3, pp. 1050–1063, 2012.

[10] A. Seijas-Macías and A. Oliveira, "An Approach to Distribution of the Product of Two Normal Variables," *Discussiones Mathematicae Probability and Statistics*, vol. 32, no. 1-2, pp. 87–99, 2012.

[11] M. M. Azari, F. Rosas, K.-C. Chen, and S. Pollin, "Ultra Reliable UAV Communication Using Altitude and Cooperation Diversity," *IEEE Trans. Commun.*, vol. 66, no. 1, pp. 330–344, 2017.

Fig. 4: Relative errors between exact and approximate curves with K-factors, outage probabilities, and number of PRUs.